

To ablate the second arch crest stream, we removed rhombomere 4 and portions of the adjacent rhombomeres 3 and 5 at stage 9/10. Later hindbrain ablations were performed at stage 12, the whole neural tube was removed at the level of rhombomere 4 using a fire-sharpened tungsten needle, and the embryos were reincubated for 24 hours.

14. E. Veitch, J. Begbie, T. F. Schilling, M. M. Smith, A. Graham, *Curr. Biol.* **9**, 1481 (1999).
15. K. W. Tosney, *Dev. Biol.* **89**, 13 (1982).
16. A. Lumsden, R. Keynes, *Nature* **337**, 424 (1989).
17. H. Simon, S. Guthrie, A. Lumsden, *J. Neurobiol.* **25**, 1129 (1994).
18. D. M. Noden, *Dev. Biol.* **96**, 144 (1983).
19. A. Graham, I. Heyman, A. Lumsden, *Development* **119**, 233 (1993).
20. T. Piotrowski, C. Nusslein-Volhard, *Dev. Biol.* **225**, 339 (2000).
21. P. Trainor, R. Krumlauf, *Nature Cell Biol.* **2**, 96 (2000).
22. N. Horigome *et al.*, *Dev. Biol.* **207**, 287 (1999).
23. L. A. Barlow, R. G. Northcutt, *Development* **124**, 949 (1997).
24. We thank P. Scotting for the *Sox-10* probe and A. Lumsden for critical comments on this manuscript. This work was funded by the UK MRC.

27 April 2001; accepted 2 August 2001

Crystal Structure of an Early Protein-RNA Assembly Complex of the Signal Recognition Particle

Klemens Wild,^{1*} Irmgard Sinning,¹ Stephen Cusack²

The signal recognition particle (SRP) is a universally conserved ribonucleoprotein complex that mediates the cotranslational targeting of secretory and membrane proteins to cellular membranes. A crucial early step in SRP assembly in archaea and eukarya is the binding of protein SRP19 to specific sites on SRP RNA. Here we report the 1.8 angstrom resolution crystal structure of human SRP19 in complex with its primary binding site on helix 6 of SRP RNA, which consists of a stem-loop structure closed by an unusual GGAG tetraloop. Protein-RNA interactions are mediated by the specific recognition of a widened major groove and the tetraloop without any direct protein-base contacts and include a complex network of highly ordered water molecules. A model of the assembly of the SRP core comprising SRP19, SRP54, and SRP RNA based on crystallographic and biochemical data is proposed.

Proteins that are inserted in or transported through membranes contain an NH₂-terminal signal sequence, which is cotranslationally recognized by the universally conserved signal recognition particle (SRP) (1). SRP is a cytoplasmic ribonucleoprotein particle (RNP) that binds the signal sequence as it emerges from the ribosome and targets the nascent chain-ribosome complex to the endoplasmic reticulum (ER) in eukaryotes or to the plasma membrane in prokaryotes (2).

In higher eukaryotes, SRP contains six proteins and can be split into two domains—the *Alu* domain and the *S* domain—that are linked by the SRP RNA consisting of ~300 nucleotides (nt) (Fig. 1A) (1). Whereas the *Alu* domain is responsible for retarding the ribosomal elongation of the nascent chain during targeting, the *S* domain forms the functional core by binding to the signal sequence and mediating the docking to the translocation machinery in the ER membrane in a guanosine 5'-triphosphate (GTP)-dependent process (1). The *S* domain consists of the

four larger proteins SRP19, the GTPase SRP54, and the SRP68/72 heterodimer, as well as the central part of the SRP RNA.

SRP19 is an essential player in the assembly of SRP (3) and binds to free SRP RNA already in the nucleolus (4). This early assembly event is a prerequisite for the binding of SRP54 to helix 8 of SRP RNA in eukaryotes (3) and involves an SRP19-induced conformational change in the RNA (5). Genome-based sequence alignments indicate that SRP19 homologs are present only in organisms whose SRP RNA contains helix 6 (6), which has been identified as the primary binding site of SRP19 (7). Helix 6 is closed by a tetranucleotide hairpin loop (tetraloop) of the unusual GNAR (N: any nucleotide, R: either G or A) sequence fingerprint (7). The adenine at the third position is strictly conserved and has been shown to be essential for SRP19 binding (7). Little structural information is available about how SRP19 binds to and reorganizes the SRP RNA to form an SRP core particle. Here we present the 1.8 Å resolution crystal structure of the human SRP19 in complex with a distal fragment of helix 6 that includes the GGAG tetraloop. Together with chemical footprint data (8, 9), the structure allows us to propose a model for the assembly of the SRP core.

To obtain crystals of the protein-RNA complex, we removed the 24 COOH-terminal residues of SRP19 that were shown to be dispens-

able for RNA binding (10) and are not conserved in the archaeal protein (6). The RNA corresponds to the same 29-nt fragment of helix 6 previously used for structure determination of the uncomplexed RNA (11), and initial, but poor, phases could therefore be obtained by the molecular replacement method. The structure was finally solved by a single-wavelength anomalous dispersion (SAD) experiment with 5-bromouridine-labeled RNA (11). Procedures are described in (12) and data and model statistics are listed in Table 1.

The structure reveals a complex protein-RNA interface in which long, presumably flexible, loops of SRP19 recognize the particular shape of the rather rigid stem-loop RNA (Fig. 1B). SRP19 is a single-domain αβ-type protein with a central three-stranded antiparallel β sheet packed on one side against two helices. It has a βαββα topology with the COOH-terminal β strand in the middle of the β sheet, similar to the K-homology (KH) domain (13), but quite different from the αβββα topology found, for example, in the double-stranded RNA binding domain (13) or in SRP9 and SRP14 (14). SRP19 sits on the tip of helix 6 with the β1 edge of the β sheet contacting the GGAG tetraloop. Two extended loop regions (L1 and L3) with short interspersed 3₁₀ helices and several conserved sequence motifs [(sequence comparisons are shown in Web fig. 1 (15)] fill the adjacent and extremely wide major groove of the RNA, which originates from a tandem A·C/C·A mismatch and a G·U wobble base pair all opening toward the major groove (Fig. 1B). Protein-RNA interactions without any direct base recognition and a complex network of highly ordered water molecules characterize the molecular interface. Previous results on the effect of mutagenesis on SRP19 binding to SRP RNA, either systematic (16) or of conserved basic residues (17), are consistent with the structure. The tight binding of SRP19 to the RNA leaves, however, the last three bases of the tetraloop, 148-GAG, solvent-exposed with the potential to form RNA-RNA tertiary interactions.

The unusual GNAR-type tetraloop is the most highly conserved region of SRP RNA helix 6 [see supplementary material (15)]. Hairpins containing tetraloops are extremely common to large RNA molecules (18) and are thought to function as nucleation sites to ensure proper RNA folding and especially RNA-RNA tertiary interactions (19). The GNRA tetraloops are most common (18) and the first atomic-

¹Biochemie-Zentrum (BZH), University of Heidelberg, Im Neuenheimer Feld 328, D-69120 Heidelberg, Germany. ²European Molecular Biology Laboratory Grenoble Outstation, BP 181, F-38042 Grenoble Cedex 9, France.

*To whom correspondence should be addressed. E-mail: klemens.wild@bzh.uni-heidelberg.de

resolution pictures of their fold and their possibility of forming RNA-RNA tertiary interactions were obtained from the hammerhead ribozyme crystal structure (20). GNRA hairpins also serve as recognition sites for protein binding, as has been shown for the antimicrobial protein ricin (21). The GNAG-type tetraloop is rare, but in the few reported cases it is involved in specific protein recognition. For example, the GAAG tetraloop capping helix 23a of 16S ribosomal RNA (rRNA) interacts with protein S15 (22) and the SL3 stem-loop recognition element of human immunodeficiency virus-type 1 (HIV-1) with a GGAG tetraloop binds to the viral nucleocapsid protein (23). The GGAG tetraloop of the human SRP RNA adopts an overall conformation similar to that of GNRA tetraloops but with some notable differences (Fig. 2). The stacking of the last three bases (148-GAG) of the loop is conserved but with G148 noticeably tilted with respect to the others (Fig. 2A), perhaps due to the stacking of the

Arg¹⁴ side chain upon it [compare Arg⁵³ of S15 stacking on the corresponding tetraloop base A728 (22)]. However, the GGAG loop adopts a much more open conformation, and water-mediated hydrogen bonds replace two of three important direct nucleotide interactions found in GNRA tetraloops (24). When superposed on the first G, the inserted water molecules displace the last three bases of the loop away from the central axis of the loop, with maximal movements of 4.3 Å for the third base and rotations of ~30° for the second and the last base (Fig. 2A). In the GAAG tetraloop of 16S rRNA, the two direct nucleotide interactions of the GNRA-type tetraloop between the first and the fourth base are retained, but the hydrogen bond between the first and the third base is lost, as in the SRP19 complex (22). Because protein S15 has rather few interactions with the tetraloop, this might represent a pseudo-free conformation of the GAAG tetraloop, suggesting that the interaction with SRP19 further distorts the helix 6 tetraloop conformation. In the GGAG tetraloop of the HIV SL3 stem-loop recognition element, the interaction with the viral nucleocapsid protein leads to complete unstacking of the tetraloop.

SRP19 binds to the tip of helix 6 with contacts, either direct or through one intervening ordered water molecule, to the backbone of nucleotides C140 to C143 and G147 to G151. The non-Watson-Crick base pairs are on the edge (U142-G155) or outside this region (tandem A:C/C:A) but contribute to the widening of the major groove which, together with the

traloop conformation, are the principle features recognized by the protein (Fig. 1B). The third base (A149) of the GGAG tetraloop of helix 6 of human SRP RNA was found to be essential for binding of human SRP19 (7) and is universally conserved in all SRP RNAs (6). This might suggest that this base would be in direct contact with the protein, but surprisingly, there are no contacts to the base of A149 at all. Only the first tetraloop base, G147, is tightly imbedded in the protein-RNA interface and makes pseudo-Watson-Crick interactions with two water molecules and the phosphate of G150 (Fig. 3A). The water molecule bound to N1 of G147 is uniquely oriented by further hydrogen bonds to residues Tyr²² and Arg³⁴, making the

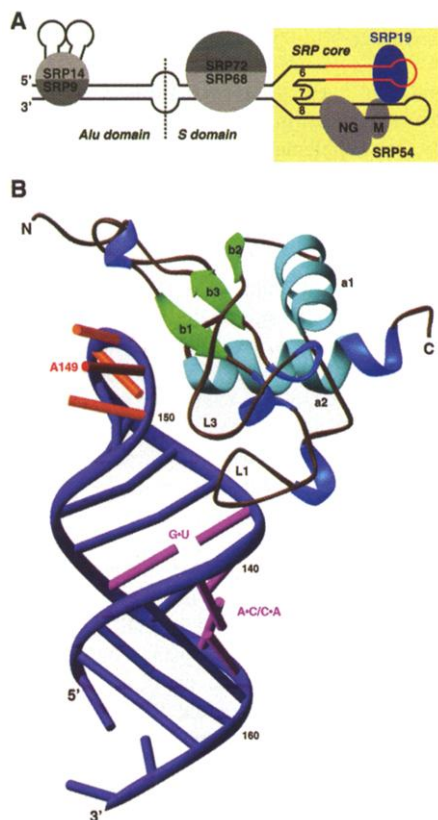


Fig. 1. (A) Schematic diagram of the human SRP19 and parts of helix 6 corresponding to the 29-nt fragment are highlighted in blue and red, respectively. The SRP core is boxed in yellow and RNA helices 6 to 8 are numbered. (B) Overall structure of the SRP19-helix 6 complex. The RNA nucleotides are reduced to color-coded cylinders. The bases of the GGAG tetraloop are highlighted in orange with the exception of the invariant A149, which is shown in red. Non-Watson-Crick base pairs of helix 6 are drawn in magenta. SRP19 is colored according to its secondary structure. Figure 1B has been prepared with the program RIBBONS (35).

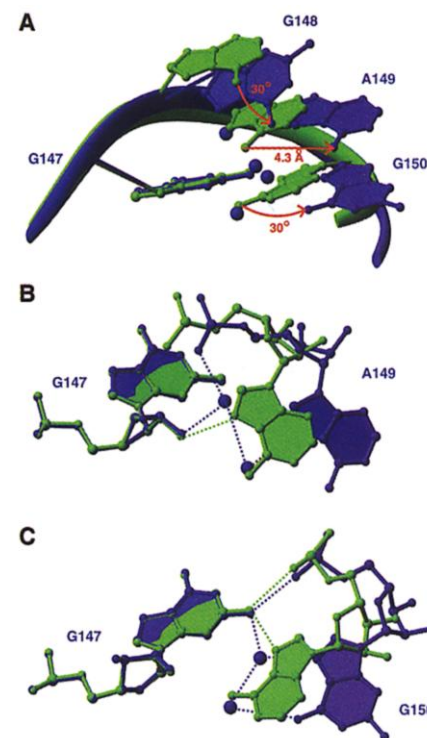


Fig. 2. Conformation and hydrogen bonding pattern of the helix 6 GGAG tetraloop compared with the GNRA type tetraloop (24). (A) Overlay of the GGAG tetraloop (blue, numbered), including relevant water molecules (blue) with the GNRA-type tetraloop (GAAA) taken from the *E. coli* SRP RNA helix 8 (green) (26). The overlay is based on the first nucleotide (G147 in helix 6). Major differences are indicated by red arrows. (B) Interaction between the strictly conserved first (G147) and the third nucleotide (A149) of SRP RNA helix 6 GGAG tetraloop. Two water molecules are inserted and replace the conserved hydrogen bond between the O2' of the first nucleotide to N7 of the third base in the GNRA tetraloop. (C) Interaction between the first and the fourth nucleotides. The hydrogen bond between N2 of the first guanine to the phosphate of the fourth nucleotide is conserved, whereas the second direct hydrogen bond between the two bases (N2 to N7 of the last base), conserved in GNRA tetraloops, is lost and two water molecules are found between the bases instead. The figure was prepared with the program RIBBONS (35).

Table 1. Structure determination, phasing, and refinement.

Data collection	
Wavelength (Å)	0.91902
Resolution (Å)	50–1.8
R_{sym}^* (%) (last shell)	8.8 (19.7)
Completeness (last shell)	91.5 (61.2)
Unique reflections	23,784
Redundancy	7.8
$I/\sigma(I)$ (last shell)	11.4 (2.7)
Phasing	
Molecular replacement†	
Correlation coefficient	24.7
R factor (%)	58.5
SAD‡	
Figure of merit	0.32
Refinement	
Resolution (Å)	50–1.8
No. of reflections (test set)	22,598 (1,142)
R_{crist}/R_{free} (%)	18.6/22.2
Number of atoms	1,829
Protein (res. § 5–118)	918
RNA (nt 135–163)	632
Water molecules	277
Mg ²⁺ ions	2
Average B factor (Å ²)	27.6
rmsd bonds (Å)	0.017
rmsd angles (°)	3.4

* $R_{sym} = \sum_{h,l} |I(h,l) - \langle I(h) \rangle| / \sum_{h,l} I(h,l)$ †Twenty to 4.0 Å resolution. ‡Fifty to 1.8 Å resolution. §res., residues. ||rmsd, root mean square deviation.

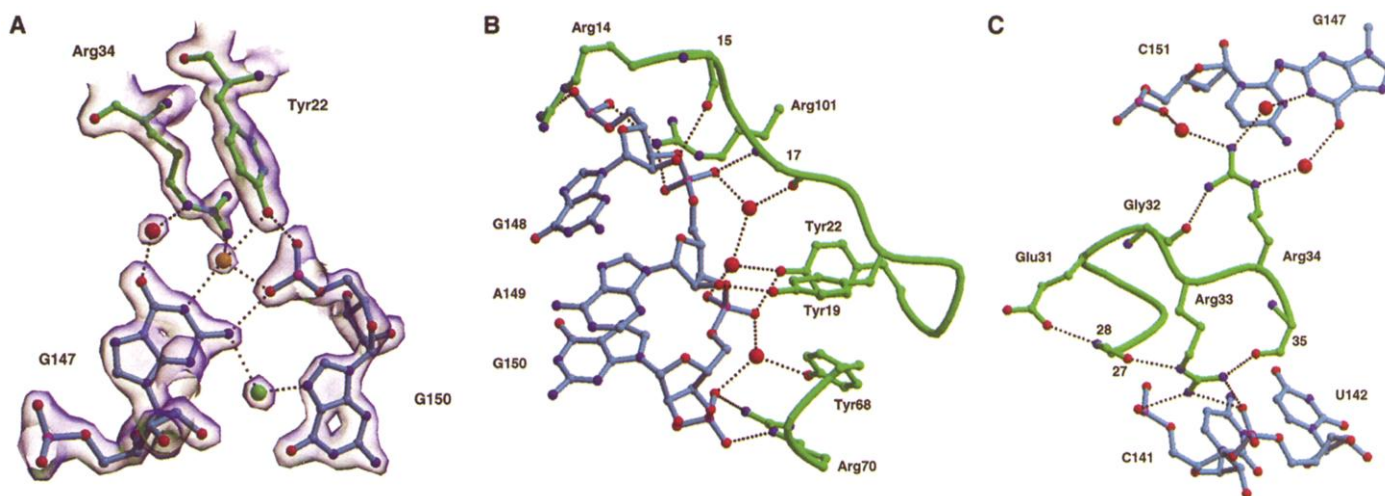


Fig. 3. Protein-RNA interactions. The protein is shown in green, the RNA in cyan, and water molecules are depicted as large red spheres (if not stated otherwise). (A) The specific recognition of the first G in the GGAG tetraloop. The final $2F_o - F_c$ electron density is shown at a 1.7σ level. The water molecule giving rise to the specific binding is shown as an orange sphere. The water molecule mediating between the first and the last base of the tetraloop is highlighted in green. (B) The recognition of the phosphoribose backbone of the GGAG tetraloop. The residues shown include the NH_2 -

terminal β sheet, the 19-YPxY sequence motif, parts of loop L3 (residues 68 to 70), and the side chains of Arg¹⁴ and Arg¹⁰¹, which stack on G148 and G147, respectively. (C) Interactions of the strictly conserved 31-EGRR fingerprint with the widened major groove. The loop region is stabilized by numerous hydrogen bonds to the protein backbone. All donor and acceptor positions of Arg³³ and Arg³⁴ are occupied (interaction between Arg³⁴-NH1 and Tyr⁶⁸-OH is not shown for clarity). The figure was prepared with the programs BOBSCRIPT (36) and Raster3D (37).

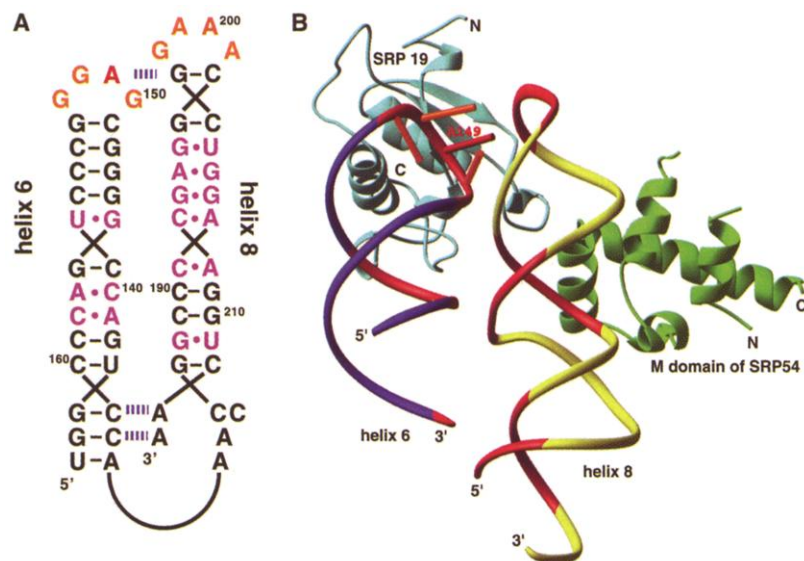


Fig. 4. Model for the human SRP core. (A) Secondary-structure model including the central and distal parts of helix 6 and helix 8 of human SRP RNA. The color coding is the same as that in Fig. 1B. Proposed interactions of unpaired adenosines with the RNA minor groove of the adjacent helix are indicated in blue. (B) Three-dimensional model of the SRP core. Chemical footprint data obtained by SRP19 binding studies (9) are highlighted in red. The superposition is based on the three distal Watson-Crick base pairs of helix 8 with three Watson-Crick base pairs of the crystal contact RNA that are in intimate contact with the SRP19-helix 6 complex (notably with the solvent-exposed bases of the GGAG tetraloop (shown as color-coded cylinders) and Lys⁶⁶ (highly conserved), Met⁶⁷, Ser⁶⁹, Arg⁷⁴, as well as Arg⁸¹ (highly conserved). Figure 4B was prepared with the program RIBBONS (35).

recognition of G147 base specific. The guanine base is further held in place by a stacking interaction with the guanidinium group of Arg¹⁰¹, which itself is interlocked between the phosphate groups of G148 and A149 (Fig. 3B). The position of Arg¹⁰¹ would sterically interfere with the conformation of a normal GNRA-type tetraloop.

All other protein-RNA contacts in the tetra-

loop region are to the phosphoribose backbone and are very often also mediated by ordered water molecules. The tetraloop backbone continues the central three-stranded antiparallel β sheet of SRP19 by forming hydrogen bonds to the protein main chain of the NH_2 -terminal β strand (Fig. 3B). Another prominent interaction feature is formed by the three conserved tyrosines Tyr¹⁹, Tyr²²,

and Tyr⁶⁸, the first two forming a YPxy sequence motif in the eukaryotic SRP19 family [see supplementary material (15)]. Like a triangular clamp, they point toward the phosphate group of G150 contributing to several direct and water-mediated hydrogen bonds and reaching also to the adjacent phosphate groups of A149 and C151 (Fig. 3B). Additionally, arginine side chains of the conserved 80-GRvr motif in the central β strand stretch over the NH_2 -terminal β strand and contribute to the protein-RNA interface (not shown).

Whereas the tetraloop docks mainly to the core of SRP19, the adjacent and extremely wide major groove of helix 6 is sensed by the two extended loops L1 (residues 19 to 45) and L3 (residues 64 to 80). The tip of loop L1, which follows the NH_2 -terminal β strand, contains the most conserved sequence motif in the SRP19 family with the fingerprint 31-EGRR (6). The high conservation is well explained by the complex organization of the motif spanning the whole major groove of the RNA (Fig. 3C). Glu³¹ and Gly³² are not involved in RNA binding but are essential for the internal loop organization. Whereas Glu³¹ forms a hydrogen bond to the main-chain nitrogen of Thr²⁸, Gly³² adopts an otherwise forbidden main-chain geometry ($121^\circ, 10^\circ$), thus positioning the following two arginines that stretch in opposite directions to span the major groove. The guanidinium group of Arg³³ is interlocked between the phosphate groups of C141 and U142 and is also hydrogen-bonded to the main-chain carbonyls of Lys²⁷ and Ile³⁵. Arg³⁴ on the other site of the groove is involved in the specific but indirect recognition of the first tetraloop nucleotide G147 and also forms water-mediated hydrogen bonds to the phosphates of G150 and C151.

Like Arg³³, it is held in place by an interaction to the protein backbone (carbonyl of Gly³²). Pro³⁶, which follows the motif, rigidifies the whole arrangement and positions the positively charged NH₂-terminal dipole of a following short 3₁₀ helix upon the phosphate groups of C141 and U142, which themselves finally are hydrogen-bonded to the main-chain nitrogens of Ile²⁹ and Ile³⁷ at the edge of the protein-RNA interface. Loop L3, located between the last two β strands, lies on top of L1, completing the enclosure of the major groove in the direction toward the tetraloop. Whereas Tyr⁶⁸ is involved in the tyrosine cluster mentioned above (Fig. 3B), the side chain of Arg⁷⁰ bridges between the carbonyl of Ala³⁰ in loop L1 and the phosphate of G151.

In summary, this structure highlights the value of high resolution in revealing the importance of highly ordered water molecules in contributing to specificity in a protein-RNA interface. It also shows that despite the plethora of examples in the recently determined ribosome structures, new modes of protein-RNA recognition remain to be discovered.

The key functions of SRP—signal sequence recognition and docking to the SRP receptor—are performed by SRP54, which in the eukaryotic SRP can only assemble to the particle after binding of SRP19 to the SRP RNA (3). The two proteins, together with their cognate RNA binding sites, therefore form the functional core of the eukaryotic SRP (25). SRP19 not only binds to helix 6, but also has a second binding site at the distal end of the highly conserved helix 8. The helix 8 binding site has been narrowed down (8, 9) to principally the 5' strand of three distal Watson-Crick base pairs adjacent to the GAAA tetraloop, the tetraloop itself, and also to parts of the highly conserved symmetrical loop not covered by the binding of the M domain of SRP54 (26). In the crystal structure of the SRP19–helix 6 complex, a symmetry-related RNA molecule is in intimate contact with both the RNA and SRP19 of the primary complex (interface of two times 950 Å). In particular, the three exposed tetraloop bases interact in the minor groove of the symmetry-related RNA molecule, and several side chains and backbone atoms from SRP19 loop L3 (residues 66 to 74) additionally contribute to form a concave surface fitting an A-RNA helix. We hypothesize that this crystal contact reveals a secondary RNA binding site of SRP19 and putative tertiary RNA-RNA interactions that could mimic the docking of helix 8 to the SRP19–helix 6 complex.

We therefore constructed a model of the functional core of the human SRP (Fig. 4) by using the observed RNA-RNA crystal contact to position, relative to the SRP19–helix 6 complex, the crystal structure of the *Escherichia coli* helix 8/*Ffh* M domain complex (26), which is homologous to the human system. The model

is plausible for the reasons summarized in (27). In particular, recent biochemical data obtained by various footprint techniques for the archaeal (8) and the human system (9) are well explained by our model, which also provides a rationale for the strict conservation of A149 in the tetraloop of helix 6. However, further studies, notably a crystal structure determination of the ternary complex SRP19–SRP54–SRP RNA, are required for confirmation of the model and for a more detailed understanding of the assembly process.

References and Notes

1. Reviewed in H. Lütcke, *Eur. J. Biochem.* **228**, 531 (1995).
2. P. Walter, A. E. Johnson, *Annu. Rev. Cell Biol.* **10**, 87 (1994).
3. P. Walter, G. Blobel, *Cell* **34**, 525 (1983).
4. J. C. Politz et al., *Proc. Natl. Acad. Sci. U.S.A.* **97**, 55 (2000).
5. K. Gowda, C. Zwieb, *Nucleic Acids Res.* **25**, 2835 (1997).
6. C. Zwieb, N. Larson, *Nucleic Acids Res.* **25**, 107 (1997).
7. C. Zwieb, *J. Biol. Chem.* **267**, 15650 (1992).
8. J. L. Diener, C. Wilson, *Biochemistry* **39**, 12862 (2000).
9. M. A. Rose, K. M. Weeks, *Nature Struct. Biol.* **8**, 515 (2001).
10. K. Römisch, J. Webb, K. Lingelbach, H. Gausepohl, B. Dobberstein, *J. Cell Biol.* **111**, 1793 (1990).
11. K. Wild, O. Weichenrieder, G. A. Leonard, S. Cusack, *Structure* **7**, 1345 (1999).
12. The 29-nt fragment corresponding to nucleotides 135 to 163 of helix 6 of human SRP RNA was in vitro transcribed by T7 RNA polymerase and purified as described previously (17). Human SRP19 was recloned without the 24 COOH-terminal residues in vector p24d(+) (Novagen) and transformed into JM109 cells. The resulting clone contains the 120 NH₂-terminal residues of SRP19 and a COOH-terminal His6-tag. The protein was purified by Ni-affinity chromatography and immediately frozen at –80°C for storage. Protein–RNA complex formation was performed in the presence of 10 mM MgCl₂ by a modified snap-cooling protocol as described (28). The complex was further purified by a MonoQ ion-exchanger (Pharmacia). Crystallization was done at a concentration of 10 mg/ml by hanging drop vapor diffusion at 18°C over a reservoir containing 50 mM sodium citrate (pH 5.6), 450 mM KCl, and 10% polyethylene glycol 3350. Initial crystals diffracted weakly to 4 Å and contained more than 30 molecules per asymmetric unit. Crystals diffracting better than 1.7 Å could be obtained after addition of 5% isopropanol and contained RNA, which was partially brominated at the C5 position of the uridines. Over 1 to 2 weeks, the crystals grew to a maximum size of 0.5 mm by 0.2 mm by 0.2 mm, belonging to space group C222₁ with a = 55.8 Å, b = 109.7 Å, and c = 89.5 Å, and one protein–RNA complex per asymmetric unit (solvent content of 55%). For cryoprotection, glycerol was added stepwise to a final concentration of 20%. Data were collected at the newly established MAD beamline ID29 at the European Synchrotron Radiation Facility (ESRF) in Grenoble, France, and processed with the HKL package (29). The structure was solved by a combination of molecular replacement (30) with a modified model of the human helix 6 RNA structure (17) and a bromine edge SAD experiment. The three bromine sites from the molecular replacement solution were refined in CNS (37), and the phase information plus density modification yielded an electron density map that finally allowed us to trace the protein with O (32). Model refinement was done with CNS. Hydrated magnesium ions were identified by their special binding sites to RNA, the short distances to their octahedrally coordinated ligands, and the peak height in the electron density (above 5σ).
13. Reviewed in J. M. Pérez-Cañadillas, G. Varani, *Curr. Opin. Struct. Biol.* **11**, 53 (2001).
14. D. Birse, U. Kapp, K. Strub, S. Cusack, A. Åberg, *EMBO J.* **16**, 3757 (1997).
15. Supplementary Web material is available on Science Online at www.sciencemag.org/cgi/content/full/294/5542/598/DC1.
16. K. Chittenden, S. D. Black, C. Zwieb, *J. Biol. Chem.* **269**, 20497 (1994).
17. S. D. Black, K. Gowda, K. Chittenden, K. P. Walker III, C. Zwieb, *Eur. J. Biochem.* **245**, 564 (1997).
18. C. R. Woese, S. Winker, R. R. Gutell, *Proc. Natl. Acad. Sci. U.S.A.* **87**, 8467 (1990).
19. O. C. Uhlenbeck, *Nature* **346**, 613 (1990).
20. H. W. Pley, K. M. Flaherty, D. B. McKay, *Nature* **372**, 111 (1994).
21. A. Gluck, Y. Endo, I. G. Wool, *J. Mol. Biol.* **226**, 411 (1992).
22. S. C. Agalarov, C. S. Prasad, P. M. Funke, C. D. Stoud, J. R. Williamson, *Science* **288**, 107 (2000).
23. R. N. De Guzman et al., *Science* **279**, 384 (1998).
24. F. M. Jucker, H. A. Heus, P. F. Yip, E. H. M. Moors, A. Pardi, *J. Mol. Biol.* **264**, 968 (1996).
25. S. Hauser, G. Bacher, B. Dobberstein, H. Lütcke, *EMBO J.* **14**, 5485 (1995).
26. R. T. Batey, R. P. Rambo, L. Lucast, B. Rha, J. A. Doudna, *Science* **287**, 1232 (2000).
27. The model is supported by the following observations. Most importantly, chemical footprint data on the ternary complex (8, 9) are well explained, notably the protection from hydroxyl radicals corresponding to nucleotides 195–UCCG in human SRP RNA, because in the model the phosphoribose backbone is completely buried. The model leads to no steric clashes, in particular between SRP19 and the M domain of SRP54. Indeed, after docking of the helix 6 and helix 8 RNAs and without any adjustment of the proteins, SRP19 and SRP54M are found to just contact each other with no overlap. There is no interference with the proposed signal sequence binding hydrophobic groove, and room is available for the missing NG domain of SRP54. Furthermore, the helix 8 tetraloop is still exposed, consistent with a possible role in interacting with the SRP receptor (33). The GGAC tetraloop interacts with the tip of helix 8 in a manner reminiscent of the GAAA tetraloop interacting with an RNA helix in the hammerhead ribozyme crystal structure (20), with the strictly conserved A149 of helix 6 forming a base triple in the minor groove of a C-G base pair. This could be the underlying rationale for the phylogenetic conservation of this base (6). In the model, helix 6 and helix 8 run side by side and parallel, consistent with their joining at a junction point. Furthermore, the chemical footprint data in the short part of the asymmetric loop region of helix 8, which has been assigned to RNA-RNA tertiary interactions (8), can be explained if unpaired adenosines in this region of helix 8 make base triples to the minor groove of helix 6. This type of interaction has been found to represent a universal mode of RNA helix packing (34) and could result in a reorganization of the asymmetric loop, which might be crucial for the subsequent binding of the M domain of SRP54.
28. S. R. Price, N. Ito, C. Oubridge, J. M. Avis, K. Nagai, *J. Mol. Biol.* **249**, 398 (1995).
29. Z. Otwinowski, W. Minor, *Methods Enzymol.* **276**, 307 (1997).
30. J. Navaza, *Acta Crystallogr. A* **50**, 157 (1994).
31. A. T. Brünger et al., *Acta Crystallogr. D* **54**, 905 (1998).
32. T. A. Jones, J. Y. Zou, S. W. Cowan, M. Kjeldgaard, *Acta Crystallogr. A* **47**, 110 (1991).
33. J. R. Jagath et al., *RNA* **7**, 293 (2001).
34. E. A. Doherty, R. T. Batey, B. Masquida, J. A. Doudna, *Nature Struct. Biol.* **8**, 339 (2001).
35. M. Carson, *J. Appl. Crystallogr.* **24**, 958 (1991).
36. R. M. Esnouf, *J. Mol. Graph.* **15**, 133 (1997).
37. E. A. Merritt, D. J. Bacon, *Methods Enzymol.* **277**, 505 (1997).
38. We thank W. Shepard and A. Thompson for assistance at beamline ID29, ESRF (Grenoble, France). K.W. was supported by the SRPNET, a research network of the European Union Framework IV Training and Mobility Research program of which I.S. and S.C. are both principal investigators (ERBFMRXCT-960035). We thank K. Strub (a principal investigator of SRPNET) for the initial clone of human SRP19. Coordinates and structure factors have been deposited in the Protein Data Bank (accession code 1JID).

27 June 2001; accepted 13 August 2001